Polymer Degradation and Stability 94 (2009) 1061–1071

Contents lists available at ScienceDirect

Polymer Degradation and Stability

journal homepage: www.elsevier.com/locate/polydegstab

Application of near infrared spectroscopy and multivariate data analysis for the evaluation of glue lines of untreated and copper azole treated laminated timber before and after ageing

Florindo Gaspar [a], João Lopes [b], Helena Cruz [c], Manfred Schwanninger [d,*], José Rodrigues [e]

[a] Polytechnic Institute of Leiria, School of Technology and Management, Morro do Lena, Alto do Vieiro, 2411-901 Leiria, Portugal
[b] REQUIMTE, Serviço de Química-Física, Faculdade de Farmácia, Universidade do Porto, Rua Aníbal Cunha 164, 4099-030 Porto, Portugal
[c] Laboratório Nacional de Engenharia Civil, Timber Structures Division, Avenida do Brazil 101, 1700-066 Lisboa, Portugal
[d] Department of Chemistry, BOKU – University of Natural Resources and Applied Life Sciences Vienna, Muthgasse 18, A-1190 Vienna, Austria
[e] Tropical Research Institute of Portugal, Forest and Forest Products Centre, Tapada da Ajuda, 1349-017 Lisboa, Portugal

ARTICLE INFO

Article history:
Received 7 December 2008
Received in revised form
3 March 2009
Accepted 6 April 2009
Available online 17 April 2009

Keywords:
Wood
Delamination
Near infrared (NIR) spectroscopy
Partial least squares regression
Copper azole
Phenol-resorcinol-formaldehyde (PRF) glue lines

ABSTRACT

The necessity for inspection and assessment of glued laminated timber structures in service has raised interest in the evaluation of the glue lines. Glue line spectra were analysed and are discussed in detail with respect to spectral contributions from the adhesive, the hardener, the wood lamella below the adhesive, the curing temperature as well as ageing-related spectral changes. The combination of near infrared (NIR) spectroscopy and principal component analysis (PCA) allowed distinguishing between aged and non-aged samples and different copper azole preservative treatment levels of phenol-resorcinol-formaldehyde (PRF) glue lines. NIR-based partial least squares (PLS) regression modelling was performed for the glue line shear strength and for the curing temperature. These findings show that NIR spectroscopy is a fast and useful technique to evaluate the degradation on the PRF glue lines of untreated and copper azole treated laminated timber.

© 2009 Elsevier Ltd. All rights reserved.

1. Introduction

Glued laminated timber structures used worldwide in buildings and bridges have been significantly applied during the last decade in Portugal. However, little is known about the durability of this type of structure, especially concerning glue line robustness. Glue line performance depends on the proper combination of preservative treatment and adhesive [1,2]; when done with phenolic adhesives they are said to be more durable than wood [3]. Nevertheless during weathering some degradation can occur [4]. Deterioration of glued joints may result from excessive loading imposed on the structural member [5], internal stresses due to shrinking and swelling of the wood [6] or chemical reaction of the adhesive with water [7] and/or other products [8]. Water, temperature, and ultraviolet light may induce degradation of the adhesives [9] and wood [10]. For wood adhesives, the most important causes of degradation are due to changes in temperature and moisture [6]. The bond properties can be altered and plasticisation, hydrolysis, cracking, or crazing may occur [4] that in the worst cases leads to delamination.

Structures in service with signs of degradation address the need to evaluate the structural integrity. Degradation and failures mainly due to errors in the design and/or construction increased the worries and the interest for this issue [11]. Moreover, glue lines made with deep treated wood have lower durability than untreated wood [2,12,13], which depends on the preservative product and treatment level used.

Besides visual inspection, no other method is so far commonly used. Non-destructive methods such as ultrasonics [14–16] have shown limitations due to the influence of wood properties and its variability on the attenuation of ultrasonic waves and on ultrasonic parameters [17]. Semi-destructive methods can be useful to have a good estimation of the strength and of the integrity without significant damage of the structure. Taking a few cores and subsequent measurement of the wood and glue line shear strength, is a reliable method [18].

* Corresponding author. Tel.: +43 1360066523; fax: +43 1360066059.
E-mail address: manfred.schwanninger@boku.ac.at (M. Schwanninger).

0141-3910/$ – see front matter © 2009 Elsevier Ltd. All rights reserved.
doi:10.1016/j.polymdegradstab.2009.04.011

Near infrared (NIR) spectroscopy, together with multivariate analysis, has been used extensively in the field of wood science, as reviewed by Workman [19] and Tsuchikawa [20]. NIR spectroscopy was used to distinguish preservative types and retentions, on Hem-fir, Douglas Fir and Eastern Hemlock, treated with CCA (chromated copper arsenate), ACZA (copper zinc arsenate) and ACQ (alkaline copper quaternary) preservatives [21] and changes due to weathering [22,23].

In this study, phenol-resorcinol-formaldehyde (PRF) glue lines of untreated and copper azole (CA) treated laminated timber samples of Maritime pine (*Pinus pinaster* Ait.) were analysed by NIR spectroscopy. The objective was to identify spectral changes of the adhesive related to ageing, preservative treatment of the wood or curing temperature that could be further used to evaluate glue lines.

2. Materials and methods

Twelve glued laminated timber beams (0.08 m × 0.12 m × 1.00 m) were prepared by gluing four lamellae for each beam. Eight beams were made from preservative-treated lamellae (32) and the remaining four were from non-treated lamellae (16). All lamellae were knife-planed less than 6 h before bonding according to EN 386 [24].

2.1. Preservative treatment

Prior to bonding, 32 out of 48 Maritime pine wood lamellae were treated with a copper azole preservative product (20.5% copper carbonate, 4.5% boric acid, and 0.45% triazole fungicides) using the empty cell process with two target retentions (16 lamellae per retention treatment) according to use classes 3 (weather exposure without ground contact) and 4 (ground contact) (EN 335-2 [25]). The treatment retention level was determined by atomic absorption spectroscopy following the standard A11 [26]. The retentions obtained were 7.6 kg/m^3 and 19.1 kg/m^3 for the lower (L) and higher (H) retention levels, respectively. The remaining 16 lamellae (Z) were not treated.

2.2. Gluing procedures

Four beams of each untreated (Z), lightly treated (L), and highly treated (H) Maritime pine lamellae were prepared with a phenol-resorcinol-formaldehyde (PRF) adhesive obtained by mixing 5:1 the liquid resin with the powder hardener. According to the manufacturer's information, the resin is composed of phenol-resorcinol-formaldehyde polymer, phenol, ethanediol, ethanol and water, whereas the hardener is composed of paraformaldehyde, wood flour, organic filler and inorganic filler. The adhesive was applied according to the manufacturer instructions using a spread rate of 500 g/m^2. During the curing time the beams were placed in a curing chamber where four alternative curing temperatures (20 °C, 30 °C, 40 °C, and 45 °C) were used (one curing temperature per beam per treatment level). The clamping pressure applied was about 0.6 N/mm^2. After 24 h, clamping was released and the beams were placed in standard conditions (20 ± 2 °C; 65 ± 5% relative humidity).

The influence of preservative treatment and curing temperature on the performance of freshly glued laminated beams was assessed by delamination tests (EN 391 [27]) and shear tests (EN 392 [28]). The procedures of these two methods are described in detail in the next two sections.

2.3. Delamination test

Principle: A gradient is introduced in the moisture content of the wood to build up internal stresses. This will result in tensile stresses perpendicular to the glue lines so that inadequate bonding quality will result in delamination of the glue lines (EN 391 [27]).

The delamination test specimens used were rectangular cuboids, according to (EN 391 [27]) taken from the beams as illustrated in Fig. 1, having the same dimensions of the cross-section of the beams (0.08 m × 0.12 m) and 0.075 m along the grain. These tests were done according to both methods A (37 specimens) and B (27 specimens), 5 or 6 specimens being used for each combination of preservative treatment and curing temperature.

The delamination test induces the degradation of the specimens, submitting them to cycles of impregnation with water using pressure inside of a cylindrical vessel followed by a fast drying period in a kiln. In method A three cycles were applied whereas for method B only two were done. The delamination was evaluated, immediately after the drying period, measuring the sum of the lengths where separation of glue lines occurred on both end-grain surfaces of each test specimen and calculating its percentage relatively to the total glue lines length. The objective of this test is to evaluate the performance of the glue lines.

For this work the importance of this test is not related with the delamination results (lengths of glue line separation) but with the chemical degradation that occurred during the delamination test. Despite being an artificial method the water intake and the drying process are also present in the natural ageing processes. The pressure and the higher temperatures used in this test simulate an accelerated ageing (weathering) compared to the natural one. Therefore similar chemical changes can occur and are expected.

The delamination test samples are hereafter called aged samples and the remaining ones non-aged.

2.4. Shear test

Shear strength (wood strength – WS and glue line strength – GS) was evaluated on 61 specimens (4–6 for each combination of preservative treatment and curing temperature) taken from the beams (Fig. 1), according to standard EN 392 [28]. After the delamination test, the specimens were cut to the standard shear specimen dimensions and also shear tested. Before the shear test all

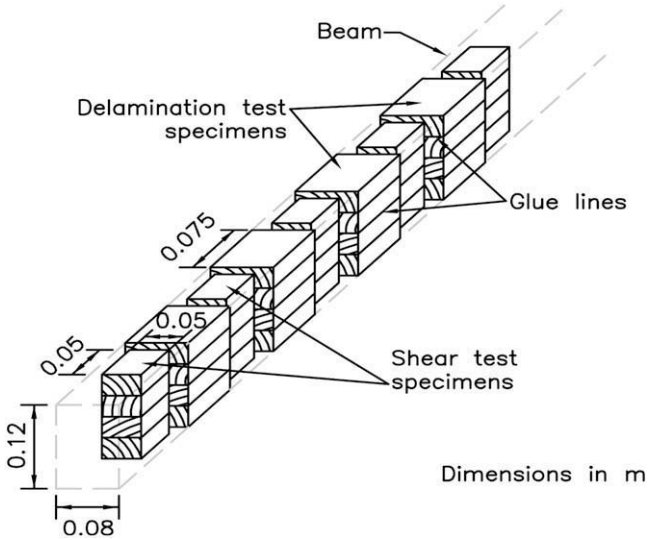

Fig. 1. Sampling plan for the beams.

specimens were conditioned to the equilibrium moisture content at approximately 65% relative humidity and 20 °C. Both the glue lines and the adjacent wood lamellae were assessed for shear strength, placing the shear plane on the glue lines or in the wood, respectively (Fig. 2).

2.5. Adhesive film

An adhesive film specimen was prepared by pressing the adhesive between glass lamellae and then cured at about 30 °C, during 24 h.

As in this study only the cured adhesive was investigated – it will only be called adhesive hereafter.

2.6. Near infrared spectroscopy

The NIR spectra of glue lines were collected, after the shear test on the exposed adhesive surface, including all combinations of treatment levels (Z, L and H), curing temperatures (20 °C, 30 °C, 40 °C, and 45 °C) and ageing. Since high wood failure percentage (WFP) was obtained during shear testing it was necessary for most of the samples to remove carefully the wood covering the glue line by using a sharp tool to obtain a flat and wood-free surface for the collection of the NIR spectra (Fig. 3). NIR spectra were collected in the wavenumber range from 10 000 cm^{-1}–5100 cm^{-1} with a Bruker Vector 22 N/I FT-NIR spectrometer (Bruker Optik GmbH, Ettlingen, Germany) in diffuse reflectance mode using a fibre optic probe. Each spectrum was obtained with 100 scans with a spectral resolution of 8 cm^{-1}. Three spectra were taken at different points of each glue line surface and averaged. The average spectra were used for the analyses. Spectra of the hardener and of the adhesive films were also obtained as described above. The penetration depth was investigated by acquiring the spectra in diffuse reflectance/transflection using a metal (steel) surface as reflector and a fibre optic probe. Spectra were processed with a Savitzky-Golay filter using a 25-point filter width and a second order polynomial [29]. The second derivative was obtained from the filtered spectra.

2.7. Mid infrared spectroscopy (MIR)

Spectra (32 scans per spectrum) of wood non-aged and aged, as well as from adhesive and the hardener were collected in the mid infrared wavenumber range from 375 to 4000 cm^{-1} at a resolution of 4 cm^{-1}. The FT-IR spectrometer Alpha-P (Bruker Optik GmbH, Ettlingen, Germany) with a diamond ATR (attenuated total reflection) accessory was used.

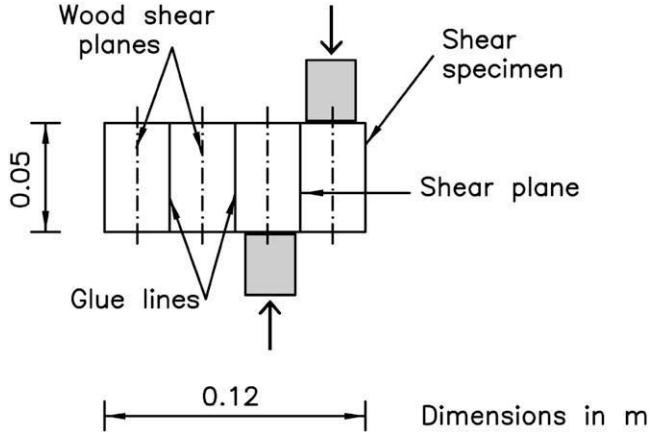

Fig. 2. A shear specimen with the shear planes for glue line and wood shear tests.

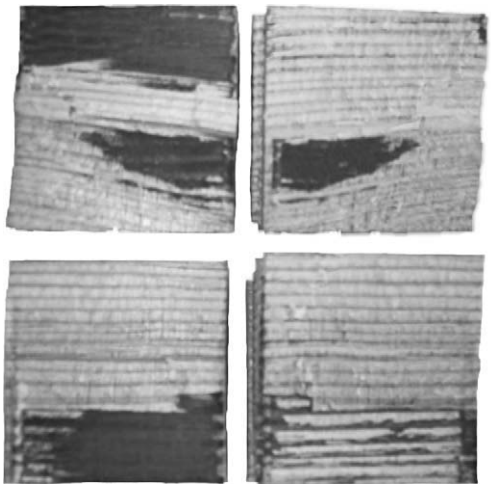

Fig. 3. Pictures of two shear tested glue lines prepared for the collection of NIR spectra.

2.8. Multivariate data analysis

Principal component analysis (PCA) and partial least squares (PLS) regression were done using Matlab version 6.5 (Mathworks, Natick, M.A.) and the PLS toolbox (Eigenvector Research, Inc. West Eaglerock Drive Wenatchee, WA).

PLS regression model validation was done using cross-validation by the "leave one out" strategy, i.e. where each sample is left out of the model formulation and predicted once, as described, e.g. by Brereton [30]. The number of principal components was selected according to the minimum root-mean-square error of cross-validation (RMSECV). Multiplicative scatter correction (MSC) was applied to minimize the undesired effect of light scattering [31].

3. Results and discussion

3.1. Near infrared spectroscopy

The NIR spectra taken from the adhesive film, untreated and preservative-treated woods, the hardener, and the glue lines (Fig. 4) as well as their second derivatives will be described in the following paragraphs, to further evaluate the contribution of each component to the glue line spectra.

3.1.1. Adhesive film

Obvious bands of the adhesive film can be seen (Fig. 4A) at about 5200 cm^{-1} corresponding to water, 5660 cm^{-1} and 5970 cm^{-1} corresponding to the first overtone of the C–H stretching and between 6090 cm^{-1} and 7200 cm^{-1} corresponding to the first overtone of N–H, O–H stretching and the C–H combination bands, the presence of water [32,33], and also contribution from the inorganic filler of the hardener at 7065 cm^{-1} [34,35].

3.1.2. Untreated wood

The NIR spectrum of the untreated wood (treatment level Z) does not show many distinct bands beside the water band (5200 cm^{-1}), the second overtone of O–H stretching and the C–H combination band range (6100–7000 cm^{-1}) and the second overtone of C–H stretching vibrations (8000–8500 cm^{-1}) (Fig. 4A). The second derivative of the NIR spectrum shows negative amplitudes at 5590, 5805 and 5887 cm^{-1} first overtone of aliphatic C–H stretching vibrations, and at 5986 cm^{-1} the first overtone of C–H stretching vibrations of the aromatic ring [36] (Fig. 4C). Bands at 6288 (from intramolecular hydrogen-bonds), 6468, 6785, and

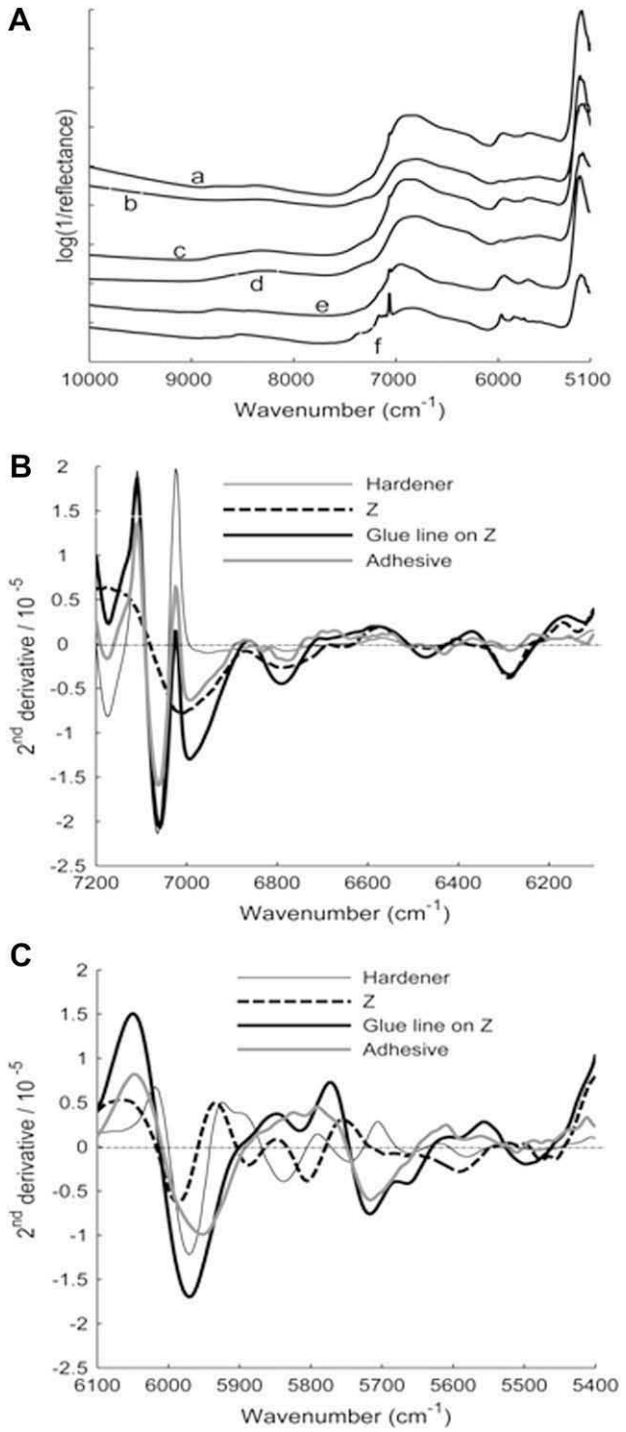

Fig. 4. A) Typical spectra from glue line, wood, adhesive and the hardener. a) Glue line on wood treatment level H; b) Wood treatment level H; c) Glue line on wood treatment level Z; d) Wood treatment level Z; e) Adhesive; f) Hardener. The spectra were shifted along the *y*-axis. Second derivatives of the spectra of the hardener, wood treatment level Z, glue line on wood treatment level Z non-aged, and adhesive. B) wavenumber range from 7200 to 6100 cm^{-1}, C) wavenumber range from 6100 to 5400 cm^{-1}. The second derivative of the hardener was divided by three.

7008 cm^{-1} in the O–H stretching vibrations range were assigned to amorphous and crystalline regions of cellulose in softwood [37]. In detail, the bands were assigned to the first overtone absorptions of OH groups in the amorphous (at about 7000 cm^{-1}), semi-crystalline (at about 6720 cm^{-1}) and to the intramolecularly hydrogen-bonded crystalline regions (at about 6290 and 6450 cm^{-1}), respectively [37]. Besides the above-mentioned OH groups from amorphous regions of cellulose, the first overtone absorptions of OH groups from hemicelluloses and lignin (aromatic and aliphatic OH groups) are also expected in this wavenumber range. The aliphatic OH groups of lignin are expected in the same range as the one from carbohydrates between 6970 and 7020 cm^{-1} and the aromatic OH groups should be found at about 6900 cm^{-1} (Fig. 4A, B). Further bands at 7309 and 7418 cm^{-1} are combinations of the first overtone of C–H stretching vibrations, and at 8304, 8560, 8640, and 8815 cm^{-1} derive from the second overtone of C–H stretching vibrations that includes the lignin aromatic and aliphatic C–H stretching vibrations between 8000 cm^{-1} and 9300 cm^{-1} [32,33].

The bands deriving from wood are of interest to evaluate the spectral contribution of wood from (i) the solid wood lamella below the adhesive and (ii) the wood flour that is part of the hardener.

3.1.3. Preservative-treated wood

The preservative treatment of wood leads to a relative decrease of the band at about 8270 cm^{-1} accompanied by shift to 8360 cm^{-1} and an increase of the slope above 7500 cm^{-1}, which was also observed by others using other preservatives [21]. Differences between the two treatment levels (Z and H) shown in Fig. 4A may also be due to preservative product composition (copper carbonate, boric acid, and triazole fungicides) that influences the spectra.

3.1.4. Hardener

The hardener shows bands near 5200 cm^{-1} (the water band), 5750, 5808, 5845, 5970 and 7065 cm^{-1} (Fig. 4A). The most intensive ones appear in the second derivative of the spectrum at 5745, 5839, 5970, 7065 and 7174 cm^{-1} (Fig. 4B,C).

The hardener bands that appear at similar wavenumbers as wood bands can be seen at 5970 cm^{-1}, corresponding to the wood band at 5986 cm^{-1} (the first overtone of the aromatic C–H stretching vibration of lignin), and at 6288 cm^{-1} (a cellulose-derived band) (Fig. 4B). The band at 5970 cm^{-1} should be mainly of aliphatic nature as, beside a small aromatic band due to a small amount of wood, no aromatic band could be seen in the MIR spectrum (not shown) of the hardener.

The presence of wood flour in the hardener should also have influence on the bands observed within the range from 6100 cm^{-1}–7200 cm^{-1}, since these can include the first overtone of the cellulose hydroxyls overlapped with the first overtone of the lignin hydroxyl vibrations [21,38]. However, in the second derivative only a few weak bands can be observed, although a broad band at about 6860 cm^{-1} can be seen in the spectrum (Fig. 4A).

In contrast, intensive bands from the inorganic part (kaolin) are visible in the MIR spectrum (not shown). The two bands at 7065 and 7174 cm^{-1} from the inorganic filler of the hardener were also found in the literature [34,35,39] and have a high absorption coefficient [39]. Due to the latter, care has to be taken not to overestimate the inorganic filler content and not to underestimate other substances in the hardener.

3.1.5. Contributions from the components to the glue line spectra

The second derivative of the spectrum of the glue line (adhesive film in brackets) shows bands at 5500 (5550), 5715 (5716), 5815, 5974 (5955), 6286 (6287), 6471, 6790 (6775), 6993 (6992), 7062 (7062), and 7172 (7175) cm^{-1} (Fig. 4B, C), and the bands not shown at 8326 and 8755 (8761) cm^{-1}. The bands related with OH groups (between 6100 and 7200 cm^{-1}) are not exclusively due to wood as also the adhesive has free OH groups [6].

Besides the preservative treatment that leads to an increase of the slope of the spectra above 7500 cm^{-1} (as mentioned earlier), also the spectra of the hardener and the adhesive film show higher slopes in this range compared to wood thus contributing to an

increase of the slope of the glue line (Fig. 4A). Furthermore, the average spectra of each treatment level show an increase of the slope above 7500 cm^{-1} with increasing curing temperature for the non-aged and aged samples except the aged samples of treatment level L (not shown). Moreover, increasing slopes were found between average spectra of the non-aged and aged samples for each treatment level with increasing temperature, which means that ageing increased the slope. Although clear influences of the treatment level, curing temperature, and ageing were observed that allowed to distinguish between or within them using the average spectra, the variation between the individual glue lines within each treatment level is high.

Due to the facts that (i) the measured materials and (ii) the wavenumber-dependent penetration depth of the infrared radiation influence a spectrum, a non-aged H sample was investigated as described under 2.5. Depending on where the glue line was broken the thickness of the remaining adhesive from which the spectra were taken varied and therefore also the spectral contribution from it as well as of the wood below. Besides a decrease of the total absorbance from a thickness of about 0.6 mm–0.2 mm, the slope above 7500 cm^{-1} decreased with the biggest decrease between 0.25 and 0.2 mm, because at a thickness of 0.2 mm almost all the wood was removed and only the adhesive that also contains a small amount of wood from the hardener remained (not shown). This is accompanied by an increase of the band at 8755 cm^{-1} and a decrease of the band at about 8390 cm^{-1}. It has to be kept in mind that an H sample was used, which means a sample with a high treatment level that shows a bigger slope than the glue line. Using an untreated sample Z the opposite is expected, meaning an increase of the slope of the spectrum in this range (cp. Fig. 4A). The OH bands decreased continuously, and the bands at 5500, 5715, 5815, 5974 and 6286 cm^{-1} started to decrease at a thickness of about 0.3 mm. Additionally the bands at 5500, 5715, 5815 and 5974 cm^{-1} shifted.

3.2. Principal component analysis (PCA)

Principal component analysis was performed with 145 average glue line spectra (47 from wood treatment level H, 49 from wood treatment level L, and 49 from untreated wood Z). The PC 1 versus PC 2 scores plot (Fig. 5) shows a separation between the three treatment levels (Z, L, and H) along PC 1, and between aged and non-aged samples in the direction of PC 2. It was possible to get satisfactory separation between wood treatment levels and between aged and non-aged samples after applying multiplicative scatter correction (MSC) that minimises the effect of light scattering as described for example by Martens and Næs [31].

Fig. 6 shows the loadings for the first and second principal component. Variables for higher wavenumbers are the most representative on the PC 1 loadings, agreeing with the evident differences in the spectra between wood treatment levels as mentioned above. On the other hand, variables corresponding to lower wavenumbers are more representative on PC 2 loadings where distinction between aged and non-aged samples occurred. The separation between the two regions can be done at 7200 cm^{-1}, including the representative band observed on PC 2 loadings at about 7065 cm^{-1} in the lower wavenumber range.

It is well known that the moisture content of a sample has a major influence on the shape of the NIR spectra [32,40]. Besides the two main hydroxyl absorbance bands in the NIR wood spectrum at about 7000 cm^{-1}, derived from the first overtone of the O–H stretching vibration, and 5200 cm^{-1}, due to a combination of O–H bending and O–H stretching, water affects almost the whole NIR range [20,41]. The water band ($\approx$5200 cm^{-1}) had an important influence on the separation of aged and non-aged samples as can

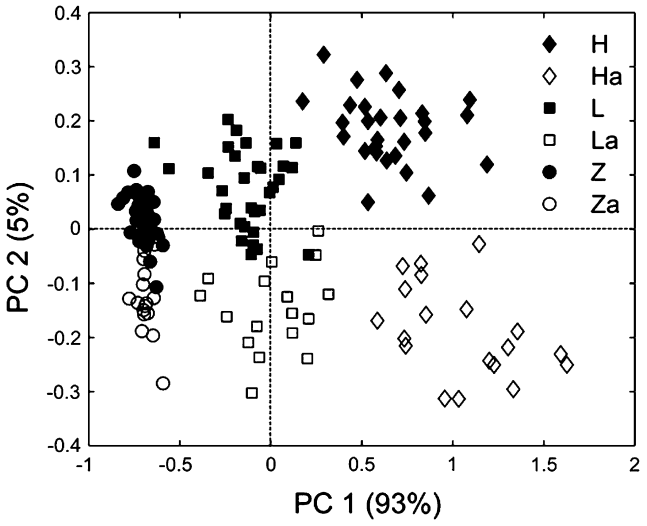

Fig. 5. Scores plot for first and second principal components using the whole spectral range with MSC scaling. H – non-aged specimens of wood treatment level H, Ha – aged specimens of wood treatment level H, L – non-aged specimens of wood treatment level L, La – aged specimens of wood treatment level L, Z – non-aged specimens of wood treatment level Z, Za – aged specimens of wood treatment level Z.

be seen in the PC 2 loadings (Fig. 6). Therefore the range below 5350 cm^{-1} was excluded from further analyses. Moreover, no influence on the separation of aged and non-aged samples was observed (not shown) after removing the range between 7000 cm^{-1} and 6850 cm^{-1} to which also water (first overtone of O–H stretching vibration at about 7000 cm^{-1}) contributes.

To see the distinction between these two regions, a PCA was done using the MSC pre-processed spectra between the two wavenumber ranges from 7200 cm^{-1}–10 000 cm^{-1} and from 5350 cm^{-1}–7200 cm^{-1}. An expected separation between the three treatment levels for higher wavenumbers but no separation according to ageing (not shown) was obtained. It may be concluded that distinction between wood treatment levels is mainly due to the absorption between 7200 cm^{-1} and 10 000 cm^{-1}, which, according to Fig. 6, is mainly due to the different slopes (cp. Fig. 4). The degree of separation decreased from H over L to Z (Fig. 5).

The separation between aged and non-aged samples was possible using the lower wavenumber range but no separation

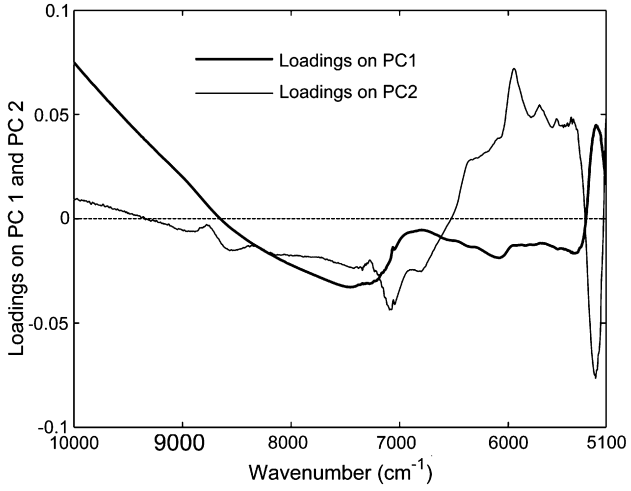

Fig. 6. Loadings for the first and second principal component using the whole spectral range with MSC scaling.

according to treatment levels was obtained. Therefore PCAs were performed using the samples of each wood treatment level separately after MSC pre-processing of the spectra. As expected a clearer separation was obtained between aged and non-aged samples using the spectral range between 5350 cm^{-1} and 7200 cm^{-1} (Fig. 7A–C). In this figure the scores have been rotated to separate along PC 1. Loadings of PC 1 for each treatment level (Fig. 8) show that the variables that separate aged and non-aged samples for the three wood treatment levels are similar. These loadings show that the aged samples have a higher-than-average number of chemical groups that are represented by the variables between 7000 cm^{-1} and 7200 cm^{-1} with an obvious band at 7065 cm^{-1} in the untreated samples Z that comes from kaolin in the hardener as seen above, being less evident for the treatment level L and not relevant for level H. Changes in this band, which derives from kaolin present in the hardener, might be due to penetration of kaolin from the adhesive into wood before curing. Depending on the treatment level the amount that penetrates into wood varies, whereas most penetrates into the untreated wood Z. During ageing the inorganic moved from the wood to the cured adhesive, which results in an increase of this band. In contrast the non-aged samples have a higher-than-average number of chemical groups that contribute to the spectra at about 5550, 5950 and 6360 cm^{-1}.

Separation between aged and non-aged samples was even possible using only the range from 7000 cm^{-1} to 7200 cm^{-1} (not shown). By using only the range from 5350 cm^{-1} to 6500 cm^{-1} to further reduce a possible influence of water, the separation decreased as expected, because not only the small difference in moisture content was removed (see 3.3) but also other information (not shown). As a rule, the distance between aged and non-aged samples was always higher for treatment level H than for L and Z for any of the wavenumber ranges used (cp. Fig. 5). Moreover, the variance explained by PC 1 (Fig. 7) follows also this order decreasing from H (85%) over L (71%) to Z (68%).

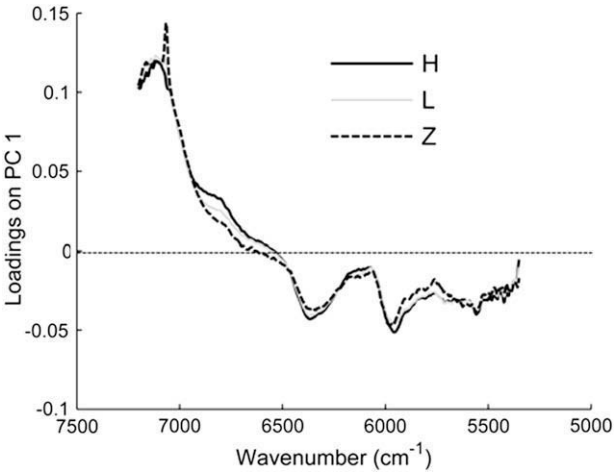

Fig. 8. PC1 loadings of each wood treatment level in the wavenumber range from 7200 to 5350 cm^{-1} of the MSC pre-processed spectra. H – wood treatment level H, L – wood treatment level L, Z – wood treatment level Z.

Despite the small influences found due to curing temperature (see 3.1.5 and 3.3) no separation in simple 2D scores plots from PCA could be obtained (the clusters are highly overlapping – not shown).

3.3. Spectral and chemical changes due to ageing

Assuming that the differences between non-aged and aged samples that led to the separation along PC 1 (Fig. 7) should also be visible in the NIR spectra, the difference spectra of the un-processed average spectra of each treatment level of non-aged and aged samples were calculated. The second derivatives of the

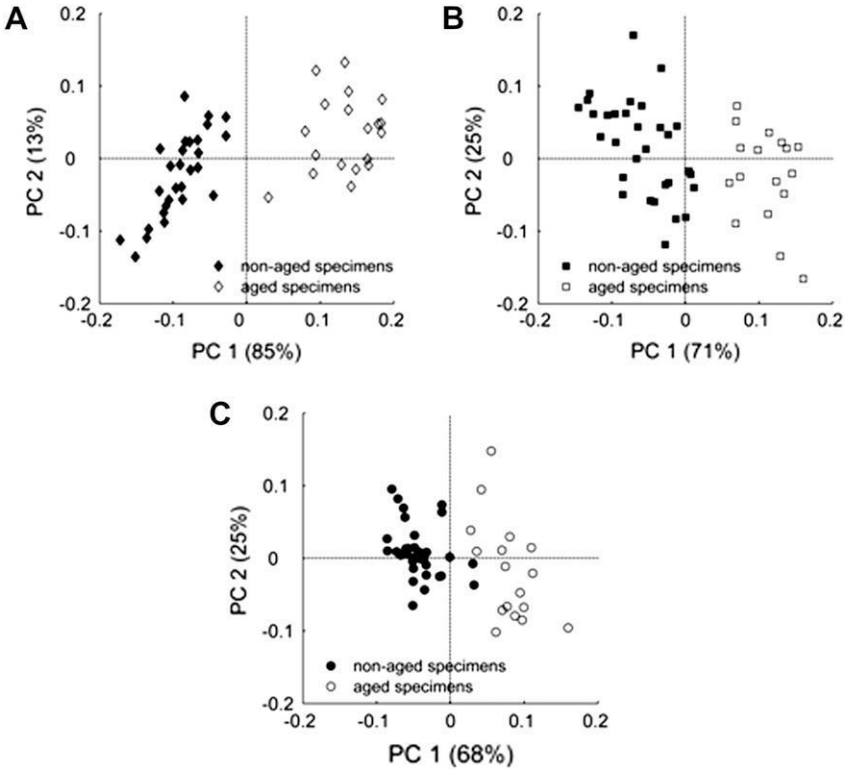

Fig. 7. First principal scores plot for each treatment level using the spectral range between 7200 and 5350 cm^{-1} with MSC scaling. A) wood treatment level H. B) wood treatment level L. C) wood treatment level Z.

difference spectra (Fig. 9) show amplitudes similar to those in the loadings of PC 1 (Fig. 8). The main difference between them is the amplitude at about 5710 cm^{-1} and that no "overshoots" at 5600, 6050, and 6475 cm^{-1} due to the calculation of the second derivatives appear in the loadings. Moreover, the difference spectra contain the full information of the chemical (and partly physical) differences between non-aged and aged samples that are not reduced to the part that focuses on their separation which is expressed by the explained variances of PC 1 (below 85%, Fig. 7).

The range between 5420 cm^{-1} and 5620 cm^{-1} including the band at 5555 cm^{-1} presented in Fig. 9B (5545 cm^{-1} in the loadings Fig. 8) indicates small differences in the moisture content. Shenk et al. [32] have assigned bands in this region to the first overtone of C–H stretching vibrations and a C–H stretching/H–O–H deformation combination in cellulose (5618 cm^{-1}), to O–H combination vibration in water (5587 cm^{-1}) and to the second overtone of O–H stretching/C–O stretching combination vibration in cellulose (5495 cm^{-1}). In fact, hydroxyl groups of the carbohydrates and lignin are the main contributors to the adsorption of water [42]. In addition, the band at 6375 cm^{-1} shown in (Fig. 9A) and at (6360 cm^{-1} in the loadings, Fig. 8) can also indicate small differences in the moisture content due to alterations of OH groups and/or their environment, which was also found by Schwanninger et al. [36] in fungi treated wood, where similar changes in the second derivatives of the NIR spectra and the PCA loadings in the range from 6250 to 6500 cm^{-1} were observed. As neither a band appears at 6360 cm^{-1} nor at 5545 cm^{-1} in the spectra of the adhesive film it can be concluded that the changes are due to changes in wood. Thygesen and Lundquist [43] found a moisture-dependent shift of the water band to higher wavenumbers with increasing moisture content. However no shift could be observed in our glue line spectra confirming that the differences found were small. Although a detailed investigation of the water band(s) as done by others [37,44] could help to reveal chemical alterations of the OH groups it is on the one hand out of the scope of this work and on the other hand very difficult to perform due to the different spectral contributions of the adhesive and the wood below.

Bands close to the band at about 5710 cm^{-1} found in the PCA loadings using all samples (Fig. 6) and in the second derivative of the difference spectra (Fig. 9B) appear only in the second derivative of the spectrum of the glue line (adhesive film) at 5715 cm^{-1} (5716 cm^{-1}) and in the second derivative of the spectrum of the hardener at 5740 cm^{-1} (Fig. 4C). This band, in the region of the first overtone of C–H stretching vibrations, possibly derives from (para-)formaldehyde that is removed during ageing in a varying degree, decreasing with the treatment level (Fig. 9B) and for all curing temperatures (not shown).

The influence of the treatment level and curing temperature can also be observed in the band that shifts from 5955 cm^{-1} (H) to 5970 cm^{-1} (Z) in the loadings plot (Fig. 8) and in the second derivative of the spectra (Fig. 9B), shifting from 5976 cm^{-1} to 5972 cm^{-1} for 20 °C and 45 °C, respectively. Bands in the range between 5900 cm^{-1} and 6100 cm^{-1} can be assigned to the first overtones of C–H stretching vibrations from methyl groups and from aryl-CH groups with the latter starting at about 5950 cm^{-1}. The lignin band appears at 5986 cm^{-1} although the second derivative of the spectrum of the glue line (adhesive film) shows a band at 5974 cm^{-1} (5955 cm^{-1}) (cp. Fig. 4B, C) and the hardener shows a band at 5970 cm^{-1}. Due to the large amount of unknown organic filler in the hardener an assignment of this band is hardly possible.

Both, the loadings (Fig. 8) and the second derivatives of the difference spectra (Fig. 9B) show a shift from 5950 cm^{-1} (H) over 5960 cm^{-1} with a shoulder at about 5985 cm^{-1} (L) to a double-band at 5966 cm^{-1} and 5988 cm^{-1} (Z). The heights of the amplitude are also different, which could explain the better separation of the non-aged and aged samples in the scores plots (Figs. 2 and 4) with the increase of the treatment level. Possible causes for this behaviour may be removal of wood-aromatics (lignin and possibly extractives) or the removal and/or chemical changes of the aromatics from the resin during ageing.

Copper and preservatives such as copper azole may have chemical interference with the adhesive cure. Copper may inhibit the curing reactions of resorcinol-formaldehyde resins [45]. Preservatives such as copper azole can decrease the curing temperature [2], accelerate the cure of phenol-resorcinol-formaldehyde resins and cause a change of the surface such as collapse [46]. The referred inhibition of the curing reaction could partly explain the hypothesis drawn about alteration/removal of the amount of resin-aromatics during ageing increasing with increasing treatment level.

As shown above (Fig. 8) the band at 7065 cm^{-1} from kaolin is highest in the loadings of the Z samples, very small in the L, and missing in the H samples. Some hypothesis can assist the interpretation of these results. A first suggestion may be the penetration of kaolin from the adhesive into wood before curing, which is higher for untreated wood because of its good penetration depth [47] and/or that the adhesive tends to react more quickly with the treated wood than with the untreated ones [2,46] and then during

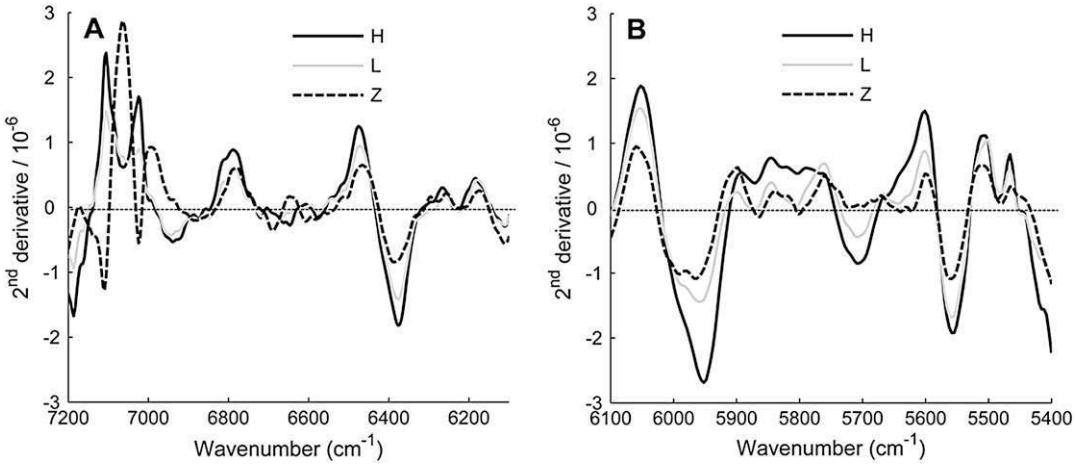

Fig. 9. Second derivatives of the difference spectra non-aged minus aged of the average spectra of all samples of each treatment level. A) wavenumber range from 7200 to 6100 cm^{-1}, B) wavenumber range from 6100 to 5400 cm^{-1}.

ageing kaolin moved from the wood to the glue line, which resulted in an increase of this band. A second one may be the chemical modification of the kaolin during ageing due to water pressure.

As a conclusion there is a significant influence of the adhesive and of the preservative treatment on the separation between aged and non-aged samples. This fact indicates that besides wood degradation, there is also a chemical modification of the adhesive behind the glue line loss of strength due to ageing (Table 1). A small increase of the glue line shear strength with increasing treatment level was observed, which was identical for all treatment levels after ageing (Table 1). Although not statistically significant, a small increase in the wood failure percentage (WFP) in the highest treatment level was observed confirming the results of Lorenz and Frihart [2]. Moreover, the enhanced performance of the glue line found by Gaspar et al. [13], namely for durability, resulting from the increase of curing temperatures could be probably a result to which a chemical change in the gluing process contributes.

3.4. Model of shear strength and curing temperature

3.4.1. Model of the shear strength

Partial least squares (PLS) [48] regression modelling for the glue line shear strength was performed for each wood treatment level (47 specimens H, and 49 specimens for each L and Z) as well as for all treatment levels together (H + L + Z) using aged and non-aged samples. Table 2 shows the cross-validation results using the MSC pre-processed spectra in the range from 10 000 cm^{-1} to 5350 cm^{-1}. The highest correlation coefficient of cross-validation (r_{CV}) was obtained for treatment level L followed by H and Z, the decrease of the root-mean-square error of cross-validation (RMSECV) and the percentage relatively to the mean shear strength (%RMSECV) shows an opposite order. The range-error-ratio (RER), suggested by Starr et al. [49], is similar for all, although H shows the highest and Z the lowest value (Table 2). The values using all samples together lay within the range of the individual treatment levels. The lower correlation coefficient obtained for the untreated wood (Z) is mainly due to the smaller range of the glue line shear strength. Nevertheless, the preservative treatment that can be seen in the spectra especially at higher wavenumbers has a significant influence on the adhesive, which agrees with the results of shear strength obtained by Gaspar et al. [18] with different specimen dimensions and preservative treatment levels.

NIR spectroscopy combined with PCR (principal component regression) or PLS regression has been used to predict mechanical wood properties such as modulus of elasticity [38,50–53], modulus of rupture [38,51], bending strength and compressive strength [52,54]. The percentage of the RMSEP (root-mean-square error of prediction) relatively to the means of modulus of elasticity and bending strength reported by Kelley et al. [38] is roughly of the same magnitude then the %RMSECV found in this study that ranges from 9% to 15%.

Although the results are promising they are still not satisfying and sources of "error" should be discussed. Besides the already mentioned varying contribution of the wood below the adhesive due to different thickness of the adhesive after shear testing, the influence of the reflection properties of the more or less rough surfaces that result after shear testing, which were tried to correct using MSC, the test [28] itself and especially the high variability of the material is a not easy to handle problem. As an example the shear strength of a glue line of an untreated wood sample Z cured at 20 °C and non-aged from which five specimen were tested gave an average shear strength of 11.2 N/mm^2 and a standard deviation of 1.41 N/mm^2, and for the same beam after ageing an average of 9.9 N/mm^2 and a standard deviation of 1.8 N/mm^2 were obtained. In addition a question arises about how representative is the value of shear strength and how representative is the area from which the spectra have been collected.

Another fact stressing these questions is that, although the spectra were collected from areas were a glue line failure appears, as a rule the shear failure does not occur only on the glue line, but on both glue line and wood. In addition the WFP was always very high (about 80%) and roughly not decreasing after the ageing process (Table 1). In fact, the final strength of a glue-bond results form the strength of the parts to be joined [55], being highly dependent on the wood shear strength [18] which also decreased during ageing (Table 1). The high wood failure percentage observed on the shear plane (Table 1) support this statement. These facts can be an explanation for the low correlation coefficients obtained (Table 2). Although the glue line spectra have been influenced by wood and adhesive composition it seem not to represent appropriately the intervenients on the glue line strength referred by Scheikl et al. [55].

3.4.2. Model of the curing temperature

Even though no clear separation from PCA could be obtained (see 3.2), PLS regression modelling was performed for the curing temperature, because an influence of the curing temperature on the MIR spectra of PRF resins was reported [56]. Although the biggest spectral changes were observed above 70 °C, some alterations were already seen between room temperature and 40 °C [56].

Several pre-processing methods and spectral ranges were investigated. The ones that gave the most uniform results are presented (Table 3), although some gave better correlation coefficients up to 0.9 for the treatment level L (not shown). The treatment level specific models are little bit more precise than the two models

Table 1
Results of the wood and the glue lines shear strength and the wood failure percentage (WFP) of each wood treatment level.

Treatment level	Non-aged samples			Aged samples		
	No. of samples[a]	Strength (N/mm^2)	WFP (%)	No. of samples[a]	Strength (N/mm^2)	WFP (%)
	Glue line					
H	48	12.1 (1.3)	79	47	10.2 (1.6)	82
L	53	12.0 (1.7)	80	41	10.3 (2.1)	79
Z	54	11.6 (1.4)	81	54	10.3 (1.6)	80
	Wood					
H	54	13.7 (0.8)	–	47	10.6 (1.7)	–
L	53	13.2 (0.7)	–	48	10.9 (2.1)	–
Z	57	11.6 (0.8)	–	51	10.0 (1.7)	–

( ) – Standard deviation.
[a] The number of samples refers to the number of wood or glue line shear planes tested.

Table 2
PLS - R cross-validation results for the glue line shear strength using the MSC pre-processed NIR spectra in the range from 10,000 cm^{-1}–5350 cm^{-1}.

Treatment level	No. of samples	No. of PCs	r_{cv}	RMSECV (N/mm^2)	RER_{cv}	%RMSECV	Range (N/mm^2)	Mean (N/mm^2)
H	47	7	0.59	1.36	5.3	12	7.2	11.8
L	49	5	0.62	1.70	4.9	15	8.3	11.7
Z	49	4	0.41	0.98	4.5	9	4.4	11.0
H + L + Z	145	4	0.55	1.49	5.2	13	7.8	11.5

No. of PCs – number of PLS components.
r_{cv} – correlation coefficient of cross-validation.
RMSECV – root-mean-square error of cross-validation.
RER_{cv} – range-error-ratio (range/RMSECV).
%RMSECV – RMSECV percentage relatively to the mean strength (RMSECV/mean*100%).
Range – maximum shear strength minus minimum shear strength.

Table 3
PLS - R cross-validation results for the curing temperature (20, 30, 40, and 45 °C, range 25 °C) using the NIR spectra in the range from 6100 cm^{-1}–5350 cm^{-1}.

Treatment level	No. of samples	Pre-processing routine	r_{cv}	RMSECV (°C)	No. of PCs
H	47	No	0.71	7.0	9
		MSC	0.69	7.1	7
L	49	No	0.72	6.4	3
		MSC	0.72	6.5	3
Z	49	No	0.69	7.1	9
		MSC	0.63	7.6	5
H + L + Z	145	No	0.63	7.3	7
		MSC	0.58	7.7	5

MSC – multiplicative scatter correction.
No. of PCs – number of PLS components.
r_{cv} – correlation coefficient of cross-validation.
RMSECV – root-mean-square error of cross-validation.

using all samples which gave correlation coefficients of about 0.6, RMSECVs near to 7.5 °C, and needing 6 PLS components in average.

Similar to the shear strength model the results are promising but not satisfying and possible reasons have already been mentioned and discussed above. Since the average spectra of each treatment level and curing temperature (not shown) show curing temperature-dependent differences for the non-aged as well as for the aged samples, better models with lower errors (RMSECV of about 5.5 °C) were obtained using only non-aged or aged samples. However, the spectral variation of the samples within each curing temperature is so big that several spectra are similar to those from other curing temperatures. Therefore the models are not precise enough for prediction and further work is needed to be able to handle the problems discussed, whereas the use of ATR-FTIR could solve the problems related to the penetration depth of the infrared radiation which should allow to focus on the adhesive of glue line.

3.5. Practical importance of the results and perspectives

When assessing the safety of glued laminated timber structures in service, it is necessary to detect and quantify physical damage and/or chemical degradation of the glue lines and its influence on strength. Visual assessment is limited because only visual degradation such as delamination on the surface can be detected. Testing cores allows assessing the glue line strength but it is a destructive test and it can only be done a few times during service life without significantly damaging the structural element. Therefore non-destructive techniques for in-situ assessment of glue lines are required.

The presented results indicate that glue line NIR spectra are sensitive to the preservative treatment retention level and to the curing temperature. Both influence the chemical changes that occurred during the ageing process, what could be the reason for the better glue lines performance with increasing curing temperatures and with decreasing preservative treatment level found in previous studies [1,2,45,46,57]. In addition, the different chemical compositions of the three preservative treatment levels detected in the NIR spectra of the glue lines mean that the treatment level can possibly be predicted through the NIR spectra of the wood, what can be useful information when evaluating the performance of structures in service. Moreover, it was also shown that delamination often seen in glued laminated timber structures not only results from mechanical stresses applied to the glue line, but it may also be due to chemical degradation of the adhesive or the wood/adhesive bond, even in the case of adhesives regarded to be highly durable.

This means that when assessing chemical degradation of glued lines, as all other methods, NIR results have to be "calibrated" by comparison with non-aged specimens of the same production run (same materials and curing conditions), collected elsewhere from less exposed parts of the same structure. The practical use of NIR results also implies the existence of sound correlations between assessed chemical deterioration and strength and stiffness loss of the glue line. This has been the aim of on-going experimental work. Promising results were obtained regarding the glue line shear strength prediction.

Using infrared spectroscopy the cores taken from the glued laminated timber structural elements can be much smaller having diameters of a few millimetres compared to the ones used for shear tests (of 35 mm). Schimleck et al. [58] demonstrated that mechanical properties of wood could be predicted by NIR from increment cores. This means that the additional collection of NIR spectra from wood would allow determining wood shear strength and to follow chemical degradation of wood due to UV-irradiation [10], biodegradation by fungi [36], to determine the chemical composition of wood [59] as well as changes due to thermal treatment [60] or chemical modification [61]. Measuring infrared spectra (preferably NIR) along the core would allow determining the chemical changes and the shear strength and therefore the penetration depth and degree of weathering and/or ageing as well as deterioration kinetic.

Further developments of NIR fibre probes that will allow measuring directly the small glue line with a thickness of about 100–200 μm will alleviate (i) to collect the spectra without any contribution from wood, (ii) to interpret the spectra drawing better conclusions on chemical changes of the glue line, and (iii) to be absolute non-destructive. Moreover, additionally using MIR ATR (attenuated total reflectance) fibre probes to collect MIR spectra will also assist the interpretation of NIR spectra and therefore chemical changes (as partly shown in this work).

Further work will focus on samples from glued laminated timbers in service and artificially aged material to follow the chemical degradation and the penetration depth of it over longer times compared to the short delamination test to be closer to the real situation. The numbers of cycles used in artificial weathering studies, well known for wood [62,63], is much higher than the ones applied in the short delamination test. The degradation of both wood and glue line can thereby be followed by infrared spectroscopy [64–67] more realistic and precisely and the current shear strength can be predicted.

This type of analysis may become a useful tool to complement current inspection/evaluation methods, towards the safety assessment of glued laminated timber structures in service. Extension to other timber species and other adhesives, as well as to other exposure/ageing conditions should therefore be considered.

4. Conclusions

The NIR spectra of glue lines taken to evaluate the glued joints of laminated timber allowed us, in combination with PCA, to distinguish between aged and non-aged samples and different copper azole preservative treatment levels of phenol-resorcinol-formaldehyde (PRF) glue lines. Separation between aged and non-aged specimens was a result of alterations in both adhesive and wood, being influenced by the level of preservative treatment. PLS regression modelling of the NIR glue line spectra performed for the glue line shear strength and the curing temperature gave promising but not satisfying results. These findings show that NIR spectra can be used to evaluate the degradation on the glue lines of untreated and copper azole treated laminated timber. Further investigations are needed to find a way to handle the problems discussed and to develop more accurate PLS regression models for the prediction of the glue line shear strength.

Acknowledgements

The work was financially supported by Fundação para a Ciência e Tecnologia (Portugal), grant holder of first author SFRH/BD/30310/2006 and the research project POCI/ECM/60089/2004.

References

[1] Lee D, Lee MJ, Son DW, Park BD. Adhesive performance of woods treated with alternative preservatives. Wood Sci Technol 2006;40:228–36.
[2] Lorenz LF, Frihart C. Adhesive bonding of wood treated with ACQ and copper azole preservatives. Forest Prod J 2006;56:90–3.
[3] Gillespie R. Evaluating durability of adhesive-bonded wood joints. In: Symposium wood adhesives – research, application and needs. Madison: Noyes Publications; 1980. p. 168–77.
[4] Davis G. Durability of adhesive joints. In: Pizzi A, Mittal K, editors. Handbook of adhesive technology. 2nd ed. New York: Marcel Dekker; 2003. p. 273–91.
[5] Giustina G. La pathologie des charpentes en bois. Paris: Editions du Moniteur; 1985.
[6] Frihart C. Wood adhesion and adhesives. In: Rowell R, editor. Handbook of wood chemistry and wood composites. Florida: CRC Press; 2005. p. 215–78.
[7] Dutkiewicz J. Hydrolytic degradation of cured urea formaldehyde resin. J Appl Polym Sci 1983;28:3313–20.
[8] Storm BK, Gwisdalski M, Lindvang D, Rann A. Investigation of degradation of structural adhesives under influence of chemicals. Macromol Symp 2005;225:205–19.
[9] Bragdon M. Behavior and design of FRP-reinforced longitudinal glulam deck bridges. MSc. Maine: University of Maine; 2002.
[10] Müller U, Rätzsch M, Schwanninger M, Steiner M, Zobl H. Yellowing and IR-changes of spruce wood as result of UV-irradiation. J Photochem Photobio B 2003;69:97–105.
[11] Hansson M, Larsen HJ. Recent failures in glulam structures and their causes. Eng Fail Anal 2005;12:808–18.
[12] Vick CB. Enhanced adhesion of melamine–urea and melamine adhesives to CCA-treated southern pine lumber. Forest Prod J 1997;47:83–7.
[13] Gaspar F. Estruturas de madeira lamelada-colada – viabilidade da utilização da madeira de pinho bravo tratada com produto preservador. MSc. Lisbon: Technical University of Lisbon; 2006.
[14] Beall F, Biernacki J. Detection of adhesion flaws in parallel laminates of lumber using acousto-ultrasonics. In: Proceedings of adhesives and bonded wood symposium: 1994; Seattle, WA; 1994. 121–130.
[15] Dill-Langer G, Aicher S. Inspection of glue-lines of glued-laminated timber by means of ultrasonic testing. In: Proceedings of the 14th international symposium on nondestructive testing of wood: 2005. Eberswalde, Germany: Shaker Verlag; 2005. p. 46–60.
[16] Sandoe M, Keenan F, Beall F, Fox S. Tension-perpendicular-to-glueline strength of hot-press and conventional glued-laminated beams. In: Meyer R, Kellogg R, editors. Structural uses of wood in adverse environments. New York: Van Nostrand Reinhold; 1982. p. 88–99.
[17] Kawamoto S, Williams R. Acoustic emission and acousto-ultrasonic techniques for wood and wood-based composites – a review. Madison: Forest Products Laboratory; 2002.
[18] Gaspar F, Cruz H, Gomes A. Evaluation of glued laminated timber structures – core extraction and shear testing. In: 10th World conference on timber engineering: June 2–5 2008; Miyazaki; 2008. p. 8.
[19] Workman JJ. Infrared and Raman spectroscopy in paper and pulp analysis. Appl Spectrosc Rev 2001;36:139–68.
[20] Tsuchikawa S. A review of recent near infrared research for wood and paper. Appl Spectrosc Rev 2007;42:43–71.
[21] So CL, Lebow ST, Groom LH, Rials TG. The application of near infrared (NIR) spectroscopy to inorganic preservative-treated wood. Wood Fiber Sci 2004;36:329–36.
[22] Zanetti M, Rials T, Rammer D. NIR monitoring of in-service wood structures. In: 2005 structures congress and the 2005 forensic engineering symposium: April 20–24, 2005. New York: American Society of Civil Engineers; 2005. p. 9.
[23] Wang X, Wacker J, Rammer D. Using NIR spectroscopy to predict weathered wood exposure times. In: Proceedings of the 9th world conference on timber engineering: 2006. Portland: Engineered Wood Products Association. p. 4, http://www.ewpa.com/Archive/2006/aug/P69.pdf; 2006. Accessed 30 Jun 2008.
[24] EN 386 Glued laminated timber - Performance requirements and minimum production requirements, vol. EN 386. European Committee for Standardization; 2001. p. 15.
[25] EN 335-2 Durability of wood and wood-based products. Definition of use classes. Part 2: application to solid woo'd, vol. EN 335-2. European Committee for Standardization; 2006.
[26] A11–93: standard method for analysis of treated wood and treating solutions by atomic absorption spectroscopy. In: American wood-Preservers' Association Book of Standards, vol. A11-93. American Wood-Preservers' Association; 1998.
[27] EN 391 Glued laminated timber. Delamination test of glue lines, vol. EN 391. European Committee for Standardization; 2001.
[28] EN 392 Glued laminated timber. Shear test of glue lines, vol. EN 392. European Committee for Standardization; 1995.
[29] Savitzky A, Golay MJE. Smoothing and differentiation of data by simplified least squares procedures. Anal Chem 1964;36:1627–39.
[30] Brereton R. Introduction to multivariate calibration in analytical chemistry. Analyst 2000;125:2125–54.
[31] Martens H, Næs T. Multivariate calibration. New York: John Wiley & Sons; 1991.
[32] Shenk JS, Workman JJ, Westerhaus MO. Application of NIR spectroscopy to Agricultural products. In: Burns DA, Ciurczak EW, editors. Handbook of near-infrared analysis. New York: Marcel Dekker Inc; 2001. p. 419–74.
[33] Williams P, Norris K. Near-infrared technology in the agricultural and food industries. 2nd ed. St. Paul: American Association of Cereal Chemists, Inc.; 2004.
[34] Armenta S, Garrigues S, de la Guardia M. Partial least squares-near infrared determination of pesticides in commercial formulations. Vib Spectrosc 2007;44:273–8.
[35] Viscarra Rossel RA, McGlynn RN, McBratney AB. Determining the composition of mineral-organic mixes using UV–Vis–NIR diffuse reflectance spectroscopy. Geoderma 2006;137:70–82.
[36] Schwanninger M, Hinterstoisser B, Gradinger C, Messner K, Fackler K. Examination of spruce wood biodegraded by *Ceriporiopsis subvermispora* using near and mid infrared spectroscopy. J Near Infrared Spectrosc 2004;12:397–409.
[37] Tsuchikawa S, Siesler HW. Near-infrared spectroscopic monitoring of the diffusion process of deuterium-labeled molecules in wood. Part I: softwood. Appl Spectrosc 2003;57:667–74.
[38] Kelley SS, Rials TG, Groom LR, So CL. Use of near infrared spectroscopy to predict the mechanical properties of six softwoods. Holzforschung 2004;58:252–60.
[39] Lindberg JD, Smith MS. Visible and near-infrared absorption-coefficients of kaolinite and related clays. Am Mineral 1974;59:274–9.
[40] Sousa-Correia C, Alves A, Rodrigues JC, Ferreira-Dias S, Abreu JM, Maxted N, et al. Oil content estimation of individual kernels of *Quercus ilex* subsp. *rotundifolia* ((Lam) O. Schwarz) acorns by Fourier transformed near infrared spectroscopy and partial least squares regression. J Near Infrared Spectrosc 2007;15:247–60.
[41] Lin J, Brown CW. Universal approach for determination of physical and chemical properties of water by Near-IR spectroscopy. Appl Spectrosc 1993;47:1720–7.
[42] Berthold J, Rinaudo M, Salmén L. Association of water to polar groups; estimations by an adsorption model for ligno-cellulosic materials. Colloid Surf A Physicochem Eng Asp 1996;112:117–29.
[43] Thygesen LG, Lundquist S-O. NIR measurement of moisture content in wood under stable temperature conditions. Part 1. Thermal effects in near infrared spectra of wood. J Near Infrared Spectrosc 2000;8:183–9.
[44] Tsuchikawa S, Tsutsumi S. Adsorptive and capillary condensed water in biological material. J Mater Sci Lett 1998;17:661–3.
[45] Miyazaki J, Nakano T. Effects of wood preservatives on adhesive properties II. Curing reaction of resorcinol-formaldehyde resin with Cu. Mokuzai Gakkaishi 2002;48:178–83.
[46] Miyazaki J, Nakano T, Hirabayashi Y, Kishino M. Effects of wood preservatives on adhesive properties of phenol-resorcinol-formaldehyde resin. Mokuzai Gakkaishi 1999;45:34–41.
[47] Yildiz S. Retention and penetration evaluation of some softwood species treated with copper azole. Build Environ 2007;42:2305–10.
[48] Geladi P, Kowalski BR. Partial least-squares regression – a tutorial. Anal Chim Acta 1986;185:1–17.
[49] Starr C, Morgan A, Smith D. An evaluation of near-infrared reflectance analysis in some plant-breeding programs. J Agr Sci 1981;97:107–18.
[50] Meder R, Thumm A, Marston D. Sawmill trial of at-line prediction of recovered lumber stiffness by NIR spectroscopy of *Pinus radiata* cants. J Near Infrared Spectrosc 2003;11:137–43.
[51] Via BK, Shupe TF, Groom LH, Stine M, So CL. Multivariate modelling of density, strength and stiffness from near infrared spectra for mature, juvenile and pith wood of longleaf pine (*Pinus palustris*). J Near Infrared Spectrosc 2003;11:365–78.
[52] Gindl W, Teischinger A, Schwanninger M, Hinterstoisser B. The relationship between near infrared spectra of radial wood surfaces and wood mechanical properties. J Near Infrared Spectrosc 2001;9:255–61.
[53] Tsuchikawa S, Hirashima Y, Sasaki Y, Ando K. Near-infrared spectroscopic study of the physical and mechanical properties of wood with meso- and micro-scale anatomical observation. Appl Spectrosc 2005;59:86–93.
[54] Hoffmeyer P, Pedersen JG. Evaluation of density and strength of Norway spruce wood by near-infrared reflectance spectroscopy. Holz Als Roh-und Werkst 1995;53:165–70.
[55] Scheikl M, Wålinder M, Pichelin F, Dunky M. Bonding process. COST Action E13-working group 2. In: Dunky M, Pizzi T, Leemput M, editors. Wood adhesion; 2002. p. 92–122.
[56] Chow S. Curing study of phenol-resorcinol-formaldehyde resins using infrared spectrometer and thermal-analysis. Holzforschung 1977;31:200–5.
[57] Miyazaki J, Nakano T. Effects of wood preservatives on adhesive properties IV – effects of preservation and incising on shear strength and delamination. Mokuzai Gakkaishi 2003;49:212–9.
[58] Schimleck LR, Jones PD, Clark A, Daniels RF, Peter GF. Near infrared spectroscopy for the nondestructive estimation of clear wood properties of *Pinus taeda* L. from the southern United States. Forest Prod J 2005;55:21–8.
[59] Gierlinger N, Jacques D, Schwanninger M, Wimmer R, Paques LE. Heartwood extractives and lignin content of different larch species (*Larix* sp.) and relationships to brown-rot decay-resistance. Trees 2004;18:230–6.
[60] Schwanninger M, Hinterstoisser B, Gierlinger N, Wimmer R, Hanger J. Application of Fourier transform near infrared spectroscopy (FT-NIR) to thermally modified wood. Holz Als Roh-und Werkst 2004;62:483–5.

[61] Stefke B, Windeisen E, Schwanninger M, Hinterstoisser B. Determination of the weight percentage gain and of the acetyl group content of acetylated wood by means of different infrared spectroscopic methods. Anal Chem 2008;80:1272–9.
[62] Hon DN-S. Weathering and photochemistry of wood. 2nd ed. New York: Marcel Dekker Inc.; 2001.
[63] Moore AK, Owen NL. Infrared spectroscopic studies of solid wood. Appl Spectrosc Rev 2001;36:65–86.
[64] Kataoka Y, Kiguchi M. Depth profiling of photo-induced degradation in wood by FT-IR microspectroscopy. J Wood Sci 2001;47:325–7.
[65] Kishino M, Nakano T. Artificial weathering of tropical woods. Part 1: changes in wettability. Holzforschung 2004;58:552–7.
[66] Kishino M, Nakano T. Artificial weathering of tropical woods. Part 2: color change. Holzforschung 2004;58:558–65.
[67] Sudiyani Y, Imamura Y, Doi S, Yamauchi S. Infrared spectroscopic investigations of weathering effects on the surface of tropical wood. J Wood Sci 2003;49:86–92.